Biophysical Journal
Article

Biophysical Society

Vesicle Fusion Mediated by Solanesol-Anchored DNA

Kristina M. Flavier[1] and Steven G. Boxer[1,*]
[1]Department of Chemistry, Stanford University, Stanford, California

ABSTRACT Fusion between two lipid bilayers is one of the central processes in cell biology, playing a key role in endocytosis, exocytosis, and vesicle transport. We have previously developed a model system that uses the hybridization of complementary DNA strands to model the formation of the SNARE four-helix bundle that mediates synaptic vesicle fusion and used it to study vesicle fusion to a tethered lipid bilayer. Using single vesicle assays, 70% of observed fusion events in the DNA-lipid system are arrested at the hemifusion stage, whereas only 5% eventually go to full fusion. This may be because the diglycerol ether that anchors the DNA in the membrane spans only half the bilayer: upon hemifusion and mixing of the outer leaflets, the DNA-lipid is free to diffuse into the target membrane and away from the vesicle. Here, we test the hypothesis that the length of the membrane anchor may impact the outcome by comparing single leaflet-spanning DNA-lipid mediated vesicle fusion with fusion mediated by DNA anchored by solanesol, a C45 isoprenoid of sufficient length to span the bilayer. When the solanesol anchor was present on the incoming vesicles, target membrane, or both, ~2–3 times as much full fusion was observed as in the DNA-lipid mediated system, as measured by lipid mixing or content transfer. These results indicate that a transmembrane anchor increases the efficiency of full fusion.

INTRODUCTION

Membrane fusion is one of the core processes in cell biology, necessary for endocytosis, exocytosis, signaling, vesicle transport, and viral entry. Upon binding of a vesicle to the target membrane, full lipid mixing and content transfer can occur as both leaflets of the vesicle bilayer merge with the target and vesicular contents are transferred across the target membrane. It is through this process that vesicles can deliver their contents or membrane components to other regions of the cell. One of the best-characterized vesicle fusion processes is that of neurotransmitter release from neurons into the synapse, a process mediated by the SNARE proteins and aided by numerous accessory proteins (1–5). Although synaptic vesicle fusion has been studied in live cells, fusion is a complex process that also benefits from the use of reductionist models and single vesicle assays to isolate and study the key intermediates (6–10).

We have previously developed a model system that utilizes lipid-anchored DNA to mediate fusion of small unilamellar vesicles (SUVs) to a tethered patch held 8 nm from a solid support (Fig. 1 *A*) (11). These target patches are created by depositing giant unilamellar vesicles (GUVs) displaying DNA-lipids onto a surface with immobilized complementary DNA sequences, anchored such that the DNA hybrids hold the membrane away from the surface (DNAs shown in *magenta* in Fig. 1, *A* and *B*). Because the target membrane is held away from the surface, both lipid mixing using a dye-labeled lipid (shown in *red* in Fig. 1, *A* and *B*), and content transfer across the target (observed by content dye dequenching, data not shown) can be observed for individual vesicles. Hybridization of complementary DNA sequences anchored on the incoming vesicle at the 3′ end and on the target at the 5′ end (shown in *blue*, Fig. 1 *A*) brings the vesicle and target membrane into close apposition and results in fusion (12–14). In this system, proximity is sufficient to induce lipid mixing and content transfer. However, in lipid mixing experiments, ~60–80% of vesicles are arrested at the hemifused state, whereas only ~5% of events proceed to eventual full fusion (Fig. 1 *A*). The DNA-lipids used in these experiments had a single-leaflet spanning diglycerol ether as anchor (see Fig. S1 for structure and Table S1 for sequences), which is only anchored in the outer leaflet of the bilayer. As seen in Fig. 1 *A*, nothing prevents diffusion of the hybridized DNA-lipids away from the vesicle into the target bilayer, and this has previously been confirmed using dye-labeled DNAs in the DNA-lipids (14). This may explain why a large percentage of vesicles

Submitted January 23, 2017, and accepted for publication May 23, 2017.
*Correspondence: sboxer@stanford.edu
Editor: Daniel Muller.
http://dx.doi.org/10.1016/j.bpj.2017.05.034

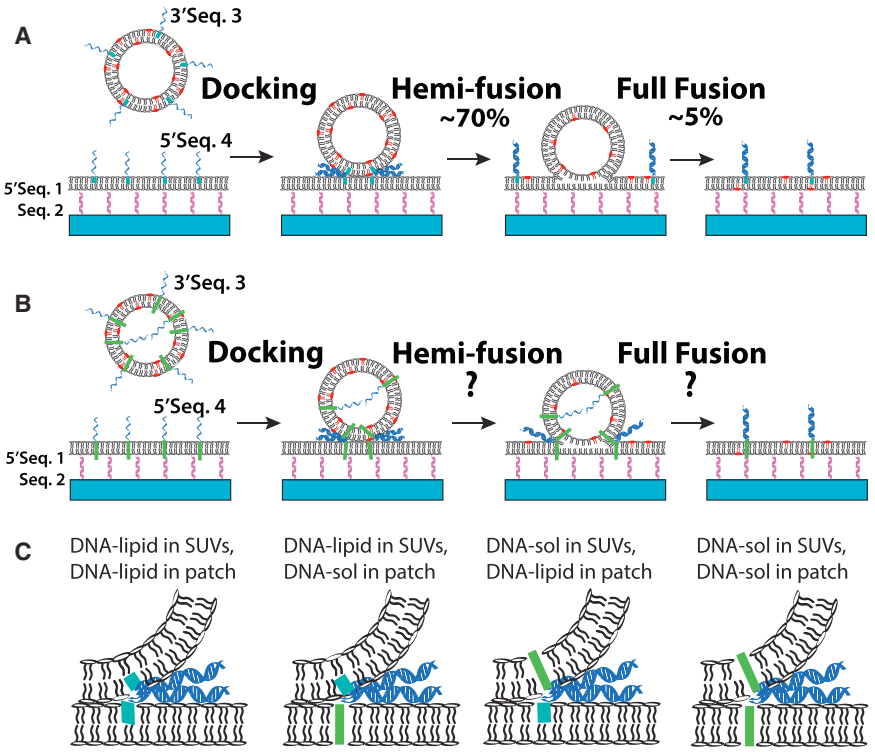

FIGURE 1 DNA-mediated vesicle fusion to tethered patches. (*A*) Given here is a schematic model of vesicle fusion mediated by hybridization of complementary DNA sequences 3′ Sequence 3 and 5′ Sequence 4 (Table S1), as studied in previous experiments (13,14). DNA is anchored by lipids spanning a single membrane leaflet and incorporated asymmetrically into vesicles. After hemifusion, the hybridized DNA can diffuse away from the vesicle. (*B*) Given here is fusion mediated by hybridization of transmembrane-anchored DNA incorporated symmetrically into membranes. The hybridized DNA remains at the site of fusion after hemifusion. (*C*) Given here are the four combinations of DNA-lipid and DNA-solanesol (DNA-sol) on incoming vesicles and target patch investigated herein. The DNA-lipid anchor is only long enough to span one leaflet of the bilayer, whereas solanesol is of sufficient length to interact with both leaflets. These four combinations are tested in Figs. 3, 4, 5, and 6. To see this figure in color, go online.

are arrested in a stable hemifusion state when the membrane anchor is an ordinary lipid. By contrast, a longer anchor that spans both leaflets might be incapable of diffusing away from the contact area between vesicle and target membrane after DNA hybridization and might increase the amount of full fusion observed (Fig. 1 *B*, where the longer anchor is shown in *green*).

The importance of a transmembrane anchor for SNARE protein function has long been a point of contention. Although formation of the SNARE four-helix bundle extends from the soluble domains to the transmembrane regions within the bilayer (2), there is conflicting evidence as to the necessity of the transmembrane domains. It is currently unknown whether the transmembrane domain serves as a passive anchor, transduces force from SNARE complex formation into the membrane, acts to disrupt the lipids at the fusion site, or promotes fusion through some other mechanism. Although several previous studies have found that replacement of the SNARE transmembrane region with a shorter anchor disfavors fusion (15–19), others have concluded that a single leaflet-spanning lipid anchor on the cytosolic SNARE domain is sufficient to allow for spontaneous fusion (7), or that a SNARE transmembrane domain used to anchor a different recognition motif does not result in full fusion in model systems (20,21).

To investigate the importance of a transmembrane anchor using our model system, we have conjugated the long-chain lipid solanesol to DNA via a disulfide linkage (Fig. 2) and use this in lipid mixing and content transfer experiments to monitor vesicle fusion to a tethered patch. Because this is a simple reductionist system, we can also explore whether the location of the solanesol anchor in the incoming vesicle and/or the target matters (Fig. 1 *C*). Although other anchors were also considered, synthetic and analytical difficulties limited our work to the solanesol anchor; these alternatives are briefly summarized in the Supporting Material for the benefit of others who may pursue this further.

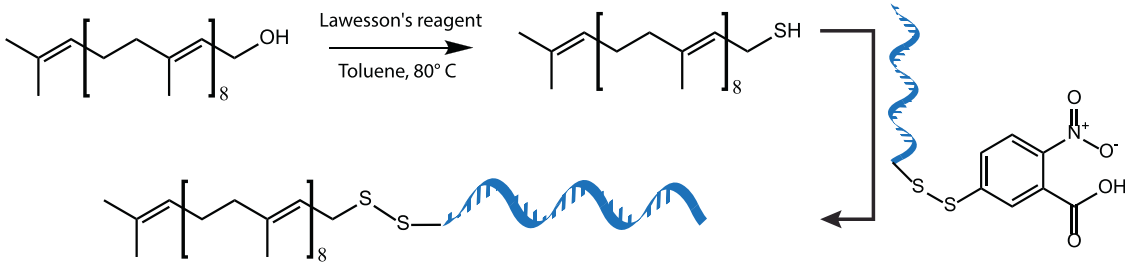

FIGURE 2 Synthesis of DNA-solanesol via thionation of solanesol followed by thiol-disulfide exchange. To see this figure in color, go online.

MATERIALS AND METHODS

Reagents

Solanesol was purchased from Sigma-Aldrich (St. Louis, MO) and TCI America (Portland, OR). Lawesson's reagent and Ellman's reagent were obtained from Sigma-Aldrich. Anhydrous toluene was obtained from a solvent still. Hexane and ethyl acetate were purchased from Thermo Fisher Scientific (Waltham, MA). DNA sequences (listed in Table S1) were synthesized by the Stanford Protein and Nucleic Acid Facility (Stanford, CA). DNA-lipids with the diglycerol ether anchor (Fig. S1) were prepared as described in Chan et al. (12).

Triethylamine acetate and the dithiol oligonucleotide modifier were obtained from Glen Research (Sterling, VA). Sodium ascorbate and copper(II) sulfate were purchased from Sigma-Aldrich. Triethyl 2,2′,2″-(4,4′,4″-nitrilotris(methylene)tris(1H-1,2,3-triazole-4,1-diyl))triacetate was generously provided by the Chidsey lab at Stanford University (22). Ethynyl phosphonic acid was synthesized in-house according to a previously published procedure (23).

L-α-phosphatidylcholine from chicken eggs, 1,2-dioleoyl-*sn*-glycero-3-phosphocholine (DOPC), 1,2-dioleoyl-*sn*-glycero-3-phosphoethanolamine (DOPE), and cholesterol were purchased from Avanti Polar Lipids (Alabaster, AL). Texas Red-DHPE and Oregon Green-DHPE were purchased from Molecular Probes (Eugene, OR). Sulforhodamine B, n-octyl glucoside, dithiothreitol, and Sepharose CL-4B resin for vesicle purification were purchased from Sigma-Aldrich.

Synthesis of thiol solanesol

To a solution of 200 mg solanesol in 2 mL toluene (0.3 mmol, 1 equivalent) was added 77 mg Lawesson's reagent (0.2 mmol, 0.6 equivalent), forming a yellow solution. The reaction mixture was stirred at 80°C overnight under positive nitrogen pressure. The thiol-solanesol product was purified via gravity column in 9:1 hexane/ethyl acetate. Clean separation between thiol solanesol and unreacted solanesol was not achieved and the product mixture was obtained as a yellow oil (201.7 mg). Product identity was verified by proton NMR. δH (300 MHz, $CDCl_3$): 1.50 (m, SH), 3.16 (2H, at, $J = 9$ Hz, CH_2SH). Only those thiol solanesol peaks distinct from the corresponding peaks in unreacted solanesol are listed. Thiol solanesol was used for further reactions within 5 days of synthesis.

Synthesis of activated thiol-DNA

DNA containing a terminal C6 S-S modifier (480 nmol) was dissolved in 1 mL aqueous sodium bicarbonate containing 100 mM dithiothreitol and stirred at room temperature for 90 min. The crude product was purified via PD-10 desalting column and eluted with pH 6.0 phosphate-buffered saline (PBS, 10 mM phosphate and 240 mM sodium chloride). Approximately 3 mL of eluent were collected, to which Ellman's reagent (14 mg) was added to a final concentration of 10 mM. The reaction mixture was incubated at room temperature for 1 h, then purified via PD-10 desalting column. 220 nmol activated thiol-DNA was obtained (46% yield), as measured by absorbance at 260 nm, and purity was verified by HPLC and MALDI-TOF.

Conjugation of thiol solanesol to activated thiol-DNA

To a solution of activated thiol-DNA in 300 μL water (200 nmol, 1 equivalent) was added octyl glucoside to a final concentration of 1%, followed by 1.2 mg thiol-solanesol (2.0 μmol, 10 equivalent). Within 1 h, the reaction mixture was observed to turn yellow as the disulfide exchange proceeded and TNB^{2-} was released. The reaction mixture was stirred overnight at room temperature. The product was purified by HPLC and obtained as a white powder (19 nmol, 10% yield). Product identity was verified by MALDI-TOF.

Purification and characterization

HPLC purification was carried out on a model No. 1260 Infinity system (Agilent Technologies, Santa Clara, CA). DNA was purified on a Poroshell C18 analytical column (Agilent Technologies) at 1 mL/min. Solvent A was 50 mM triethylamine acetate in water, and solvent B was acetonitrile. Gradient was from 5 to 100% B over 30 min. DNA-thiol solanesol was purified on a Kromasil 300 Å C4 semiprep column (Sigma-Aldrich) at 2 mL/min using the same mobile phases and gradient.

Negative ion MALDI spectra were obtained on a MALDI Microflex LRF in linear TOF mode and peaks referenced to the oligonucleotide calibration standard (Bruker, Billerica, MA). DNA-solanesol samples were spotted in 3-hydroxypicolinic acid dissolved in 50:50 acetonitrile/0.1% aqueous TFA containing 1 mg/mL ammonium citrate, for spectra showing disulfide fragmentation, or 2,4,6-trihydroxyacetophenone dissolved in 50:50 acetonitrile/50 mM ammonium citrate in water for unfragmented spectra.

NMR spectra were recorded on an Inova 300 (Coherent, Santa Clara, CA). Spectra were referenced using the undeuterated solvent peak as standard. The following abbreviations for splitting are used: m, multiplet; t, triplet; and a, apparent.

DNA-displaying vesicles

SUVs for lipid mixing experiments were formed by the extrusion method (24). DNA-lipid or DNA-solanesol (0.5 mol %) was dried down in a glass vial under stream of nitrogen. The DNA-lipids were then redissolved in chloroform and 10 μL 2:1:1 DOPC/DOPE/cholesterol at 10 mg/mL in chloroform was added (0.1 mg), followed by 4 μL Texas Red-DHPE at 1 mg/mL in chloroform (2 mol %). The mixture was dried down under stream of nitrogen and under vacuum for at least 2 h. Lipid films were rehydrated with 250 μL pH 7.4 PBS and extruded through a 30-nm polycarbonate filter for an average vesicle diameter of ~50 nm (14). SUVs with 0.5 mol % DNA-solanesol included in the lipid mixture were found to display an average of 21 $\pm$ 12 DNA on the vesicle surface, whereas SUVs with 0.5 mol % DNA-lipid included in the lipid mixture were found to display an average of 14 $\pm$ 7 DNA on the vesicle surface (see the Supporting Material; note that these ranges reflect the convolution of actual DNA number variations, variations in vesicle sizes, and measurement error). SUVs were stored at 4°C and used for up to 1 week after hydration. Note that DNA-lipid conjugates can be dispersed in buffer and then added to preformed vesicles, resulting in their incorporation only in the outer leaflet (Fig. 1 *A*). The same method does not result in quantitative incorporation of the DNA-solanesol conjugate into vesicles, and so DNA-solanesol is added to the lipid mixture before SUV formation. For these comparative experiments, DNA-lipid conjugates and DNA-solanesol conjugates were incorporated into the lipid mixture in the same manner, so they are expected to be found orientated both toward the outside and inside of the SUVs (Fig. 1 *B*).

SUVs for content transfer experiments were prepared similarly to those used for lipid mixing experiments, save that no lipid dye was added and vesicles were instead rehydrated in 250 μL 50:50 pH 7.4 PBS/90 mM sulforhodamine B (SRB) in water. Vesicles containing SRB were stored at 4°C for up to 1 week. Before content transfer experiments, vesicle were purified on a Sepharose CL-4B column in PBS to remove excess SRB. Purified vesicles were used in experiments conducted the same day to minimize dye leakage.

GUVs for tethered patches were formed via the gentle hydration method. The appropriate amounts of DNA-lipid for patch formation and DNA-lipid or DNA-solanesol for fusion desired in the final GUVs were dried down in a glass vial under a stream of nitrogen, equivalent to 0.5 mol % of 5′ Sequence 1 to tether and 0.5 mol % of 5′ Sequence 4 to fuse. The DNA-lipids were redissolved in chloroform and 10 μL 2:1:1 DOPC/DOPE/cholesterol at 10 mg/mL in chloroform added (0.1 mg), followed by 80 μL OG-DHPE at 0.01 mg/mL in chloroform (0.5 mol %). The lipid mixture was then dried under a stream of nitrogen and under vacuum for at least 3 h. To the lipid film was added 200 μL of 500 mM sucrose and

the lipids incubated at 37°C for 1 h. After preincubation, another 2 mL 500 mM sucrose was added and the GUVs were formed by 5-h incubation at 37°C on a platform shaker. The number of DNAs displayed on GUVs with 0.5 mol % DNA-solanesol added to the lipid mixture was found to be approximately equivalent to that expected for 0.08 mol % DNA-lipid (see the Supporting Material). GUVs were stored at 4°C and used for up to 1 week after hydration. Note that the gentle hydration method can produce multilamellar GUVs; however, the patch formation process liberates any internal components. Also, because the DNA lipids are added before GUV formation, DNA is presumed to be displayed on both sides of the patch; however, for clarity, this is not shown in Fig. 1, *A* and *B*.

Fusion experiments to a tethered patch

DNA-functionalized slides for formation of tethered lipid bilayers were prepared on glass coverslips within perfusion chamber gaskets (Invitrogen, Carlsbad, California) as previously described in Chung et al. (11), save that the final rinses of the slide after conjugation of 5′ alkyne-modified Sequence 2 to the surface were done with 500 mL water and 500 mL PBS. To each chamber was added 200 μL pH 7.4 PBS and 20 μL of 0.05 mg/mL GUVs containing 0.5 mol % of 5′ Sequence 1 to tether. GUVs were incubated for 20 min and visualized with epifluorescence microscopy. Upon location of a tethered GUV large enough for patch formation, the GUV was ruptured and the chamber was rinsed at least five times with 200 μL PBS. OG-DHPE in the patch was used to visualize patch integrity via uniformity of fluorescence and absence of irregular structures. Patches were also tested for nonspecific binding and fusion by addition of SUVs containing no DNA to the patch.

For lipid mixing and content transfer experiments, 10 μL of 0.04 mg/mL SUVs containing DNA-lipid or DNA-solanesol were added above each patch and a fusion stream recorded. Data was collected only from fusion events at least 5 μm away from the edge of the patch to avoid edge effects and away from any visible bilayer defects.

Microscopy

Microscopy experiments utilized an epifluorescence microscope (Eclipse TI-U inverted microscope; Nikon, Melville, NY) equipped with a 100× oil immersion objective (NA = 1.49; Nikon) with a Lumencor Spectra-X LED Light Engine (http://lumencor.com/products/spectra-x-light-engine/) as the light source. Images were recorded using an iXon 897 EMCCD camera with the MetaMorph software (Andor Technology, South Windsor, CT). For vesicle fusion experiments, a typical movie was recorded for 1000 frames at 100 ms per frame. Individual vesicle fusion outcomes were manually analyzed using the fluorescence traces generated by the MetaMorph software (14).

RESULTS AND DISCUSSION

Synthesis of DNA-solanesol

As a C45 polyisoprenoid of sufficient length to span the bilayer, solanesol is one of the most appealing options for a potential transmembrane anchor. Following a previously published procedure for allylic alcohol thionation with Lawesson's reagent (25), the solanesol hydroxyl was converted to a reactive thiol for reaction with thiol-DNA activated by conjugation to a nitrobenzoic-acid-leaving group (Fig. 2). Thiol solanesol was observed to coelute with solanesol during column chromatography and a fully pure product was not obtained. Due to the possible formation of thionated regioisomers, ^{1}H NMR was used to determine the product composition, and the product mixture was found to contain <1% tertiary thiol (Fig. S5).

Conjugation of activated thiol-DNA to thiol solanesol proceeded smoothly in 1% octyl glucoside and reaction progress was monitored by absorbance at 412 nm, corresponding to release of the TNB^{2-} leaving group from DNA. HPLC purification gave a clean separation of DNA-solanesol from the starting materials and the product was obtained in 10% yield (Fig. S6). Product identity was confirmed by MALDI-TOF with 3-hydroxypicolinic acid initially used as the matrix: due to disulfide fragmentation, which is known to occur in 3-hydroxypicolinic acid at high laser intensities (26), the spectrum contained peaks corresponding to both DNA-solanesol and reduced thiol-DNA (Fig. S7 A). Fragmentation was not observed in MALDI spectra run in 2,4,6-trihydroxyacetophenone, and the only peak present displays the *m*/*z* expected for DNA-solanesol (Fig. S7 B). Taken together, these two spectra confirm the product identity as solanesol conjugated to DNA via a disulfide linkage, and thiol-DNA is only observed upon disulfide fragmentation. With the solanesol-anchored DNA in hand, we then proceeded to investigate its membrane properties and ability to mediate fusion. We note that other strategies produced conjugates that were found to be unstable during fluorescence imaging. These are described briefly in Supporting Material.

Vesicle fusion observed by lipid mixing

Vesicle fusion to a tethered patch mediated by solanesol-anchored DNA was studied using two different assays: lipid mixing and content transfer. Lipid mixing experiments were conducted with incoming vesicles containing Texas Red-DHPE, where vesicle docking was indicated by appearance of Texas Red fluorescence puncta upon the tethered patch (14). Upon vesicle fusion to the underlying membrane, the lipid dye diffuses into the target membrane. A total loss of fluorescence indicates that the vesicle has undergone full fusion, whereas a partial loss of fluorescence corresponds to hemifusion. A two-step drop in fluorescence corresponds to the two-step process of hemi- and then full fusion (Fig. 1 *A*).

In previous fusion experiments with single leaflet-spanning DNA-lipids on both the incoming vesicles and the tethered patch target, hemifusion was the predominant outcome, with 60–80% of all fusion events stopping at hemifusion without proceeding to eventual full fusion (14). We postulated that this is in part due to the lipid anchor used, which spans only a single leaflet of the bilayer: upon hemifusion, the hybridized DNA-lipids are capable of diffusing away from the vesicle, a behavior that has been confirmed by monitoring fusion using dye-labeled DNA-lipids. With a transmembrane anchor, the hybridized DNA is expected to remain at the site between the vesicle and target membrane even after hemifusion.

Lipid mixing experiments with DNA-solanesol were set up so as to give a direct comparison to fusion conducted with shorter DNA-lipids alone. In contrast to earlier studies with the shorter DNA-lipid (12,14), both DNA-lipids and DNA-solanesol were incorporated into the lipid mixture before rehydration and extrusion, such that DNA is expected to be displayed both inside and on the outer surface of the vesicle in all cases for the closest possible comparison. Four configurations were studied in total: DNA-lipid on both vesicles and target patch; DNA-lipid on vesicles and DNA-solanesol on target patch; DNA-solanesol on vesicles and DNA-lipid on target patch; and DNA-solanesol on both vesicles and target patch (Fig. 1 *C*). Although incorporation of DNA-solanesol into only one membrane is sufficient to increase the efficiency of eventual full fusion, we also observed an asymmetric effect dependent on whether the solanesol anchor was present on the vesicle or target membrane. We divide the discussion into three classes of fates for the incoming vesicle.

Full fusion

Incorporation of DNA-solanesol into vesicles, target patch, or both resulted in an increase in fast full fusion without an observed intermediate hemifusion state, as compared to fusion mediated by DNA with the shorter lipid anchor (Fig. 3). When DNA-lipid was present on both vesicles and target membrane, fast full fusion accounted for only 2% of observed fusion events. In contrast, incorporation of DNA-solanesol resulted in an increase in full fusion to 7–10% of observed events. This increase in fusion efficiency occurred regardless of whether the solanesol anchor was present on SUVs only, in tethered patches only, or both, and did not differ significantly based on which membrane contained DNA-solanesol.

Hemi- to full fusion

Whereas DNA-solanesol increased the amount of observed fast full fusion regardless of whether it was located in the vesicle or target membrane, an asymmetric effect was observed for the hemi- to full fusion outcome (Fig. 4). When a single leaflet-spanning lipid was used as the DNA anchor on both incoming vesicles and the target patch, ~2% of vesicles were observed to undergo the hemi- to full fusion transition. No increase in hemi- to full fusion was observed when DNA-solanesol was present on the target patch and DNA-lipid was used in SUVs. However, incorporation of DNA-solanesol into SUVs resulted in an increase of hemi- to full fusion to 6% of events, regardless of whether the tethered patch contained DNA-solanesol or DNA-lipid.

The observed difference in fusion outcomes may be linked to diffusion of the hybridized DNA duplex after hemifusion. When the duplex is single leaflet-anchored on the vesicle side, it is free to diffuse away into the tethered patch after hybridization and hemifusion, similar to what is observed with the purely DNA-lipid system. Due to the large size of the patch as compared to the small area occupied by hemifused vesicles, the chance that the duplex will return to a hemifused vesicle, and thus have any further influence on the fusion outcome, is exceedingly small. On the other hand, the presence of solanesol on the vesicle side prevents the complex from leaving the vesicle. When a DNA-lipid is used in the patch, the duplex is limited to diffusion within the much smaller surface area of the vesicle, where it may find its way back to the vesicle-patch interface. Duplex diffusion upon hemifusion may also explain why this asymmetry is only observed in hemi- to full fusion events: fast full fusion proceeds without a measurable hemifusion intermediate, without allowing the hybridized duplexes to leave the site of fusion, and so the length of the vesicle-side lipid anchor does not have as strong an influence. The difference observed between full fusion and hemi- to full fusion could also indicate that the two outcomes proceed via different mechanisms. Although solanesol is capable of interacting with both membrane leaflets,

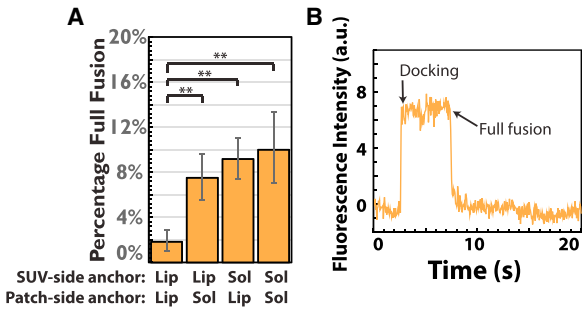

FIGURE 3 Fast full fusion with DNA-lipids and DNA-solanesol, monitored by lipid mixing. (*A*) Given here is a percent of full fusion observed when vesicles, target patch, or both contained DNA-lipids (*Lip*) or DNA-solanesol (*Sol*) (Fig. 1 *C*). n >240 vesicles for all conditions. (*B*) Given here is an example of a fluorescence trace of a full fusion event with no observed intermediate, adapted from van Lengerich et al. (14). To see this figure in color, go online.

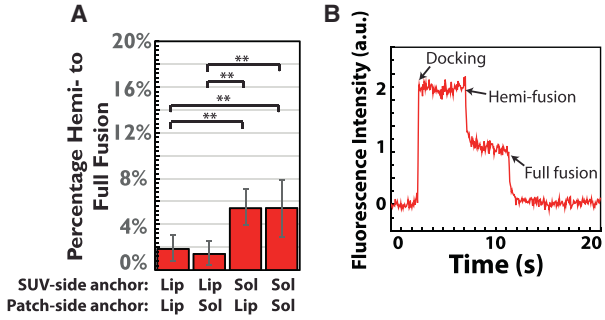

FIGURE 4 Hemi- to full fusion with DNA-lipids and DNA-solanesol, monitored by lipid mixing. (*A*) Shown here is the percent of hemi- to full fusion observed when vesicles, target patch, or both contained DNA-lipids (*Lip*) or DNA-solanesol (*Sol*) (Fig. 1 *C*). n >240 vesicles for all conditions. (*B*) Given here is an example of a fluorescence trace of a hemi- to full fusion event, adapted from van Lengerich et al. (14). To see this figure in color, go online.

potentially disrupting the distal leaflets and aiding in the opening of a fusion pore, it may also provide a source of constant tension that extends through the membrane posthemifusion, resulting in a greater percentage of eventual full fusion when compared to the shorter lipid anchor. The observed asymmetric effect on hemi- to full fusion may then be due to interaction of solanesol with the highly curved inner leaflet of the vesicle.

When conducting single-particle measurements of vesicle fusion to a tethered patch, the kinetics of transitions can be measured for individual events. The kinetics of the docking to hemifusion transition in DNA-mediated vesicle fusion have previously been studied in detail (14). When two fully overlapping 24-mer sequences were used to mediate fusion, the average time to hemifusion was ~10–13 s. For poly-A and poly-T sequences of the same length, this transition occurs more quickly, with wait times ranging from 4.8 to 9.5 s. The concentration of DNA on the vesicle surface was not shown to have a large impact on the kinetic behavior except at about an average of one DNA per vesicle, at which a slight increase in wait time was observed. Wait times for the docking to hemifusion transition showed a marked increase in DNA-solanesol-mediated fusion. When DNA-lipid was present on vesicles and DNA-solanesol in the patch, the average wait time to hemifusion was ~18 s. This increase is likely due in part to the low incorporation efficiency of DNA-solanesol into patches: although previous kinetic studies have been conducted with the target membrane containing 0.5 mol % of the DNA-lipid to fuse, only ~0.08 mol % DNA-solanesol was successfully incorporated into GUVs. The linker between the lipid anchor and the DNA sequence is also slightly longer for DNA-solanesol, which contains a C6 thiol modifier, than for DNA-lipids, where the lipid is incorporated via a phosphoramidite at the end of the DNA sequence (compare structures in Fig. 2 and Fig. S1). Although the C6 linker is relatively short, introduction of a linker between DNA and the lipid anchor has previously been shown to slow the fusion kinetics (27). In addition to the slightly longer linker, the solanesol anchor itself may also slow the docking to hemifusion transition: when DNA-solanesol was present on vesicles, regardless of whether the target patch contained DNA-solanesol or DNA-lipid, wait times increased to >30 s. Use of the solanesol anchor with the longer linker seems to greatly slow the docking to hemifusion transition, even as it encourages the transition from hemi- to full fusion.

Eventual full fusion

Taken together, when DNA-lipids are present on both incoming vesicles and target patch, ~4% of observed events proceed to eventual full fusion (Fig. 5). Although these studies utilize vesicles with DNA protruding to both the interior and exterior of the SUVs to be directly comparable with the DNA-solanesol data, this is consistent with the ~5% eventual full fusion observed in previous studies

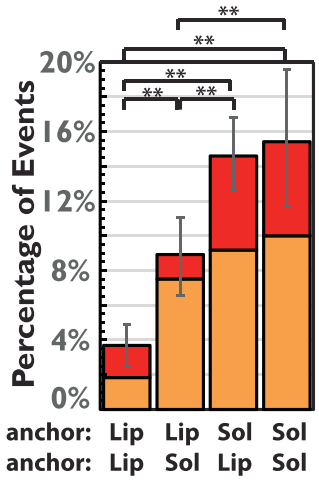

FIGURE 5 Eventual full fusion—a combination of full fusion (Fig. 3 *A*) and hemi- to full fusion (Fig. 4 *A*) mediated by DNA-lipids (*Lip*) and DNA-solanesol (*Sol*) (Fig. 1 *C*), monitored by lipid mixing. n >240 vesicles for all conditions. To see this figure in color, go online.

when DNA-lipids are displayed only on the outside of incoming vesicles. When DNA-solanesol is present in the tethered patch only, eventual full fusion accounts for 9% of observed events. When DNA-solanesol is incorporated into vesicles, 14% of events proceed to full fusion, regardless of the membrane anchor used on the tethered patch, a difference that is due mainly to the increase in hemi- to full fusion.

To test whether solanesol itself could be influencing the fusion process, outside of its role as an anchor, fusion experiments were also conducted with 0.5 mol % solanesol lipid incorporated into GUVs or 0.25 mol % solanesol incorporated into SUVs, the maximum concentrations at which DNA-solanesol would be present in each membrane. Fusion experiments with these solanesol-containing membranes were mediated by single-leaflet spanning DNA lipids and did not result in a significant increase in full fusion (see the Supporting Material). Thus, the observed increase in full fusion with DNA-solanesol is assumed to be due to the longer lipid anchor.

We note that the conformation of solanesol within the bilayer is unknown and there is no direct evidence that it acts as a true membrane-spanning anchor; however, it is of sufficient length to interact with both bilayer leaflets, and the effect on fusion outcomes indicates that solanesol does not merely serve as a passive anchor. Rather, the increase in fusion efficiency may be due to the ability of the solanesol anchor to provide a source of constant tension at the interface between vesicle and target membrane that drives the merger of both inner and outer leaflets. The asymmetric increase in hemi- to full fusion may be due to the inability of hybridized duplexes to diffuse away from the hemifusion site when a long-chain anchor is present on vesicles, though it may also be indicative that fast

full fusion and hemi- to full fusion proceed via different mechanisms.

Vesicle fusion observed by content transfer

The effect of the solanesol anchor on DNA-mediated vesicle fusion was also studied via content transfer across a tethered lipid bilayer patch. SUVs were extruded containing the content dye sulforhodamine B at self-quenching concentrations. Full fusion to a tethered patch is then accompanied by a bright burst of fluorescence corresponding to SRB dequenching, followed by complete disappearance of fluorescence as the dye diffuses away from the site of fusion (Fig. 6 *A*). With the content transfer assay, there are only two distinguishable outcomes: vesicle docking to the patch (seen as a dim fluorescent spot) and full fusion. As dye release occurs only upon full fusion, events that stop at docking cannot be distinguished from hemifusion, and hemi- to full fusion cannot be distinguished from single-step full fusion.

Key to these experiments is distinguishing true content transfer, or release of vesicle contents across a tethered patch, from vesicle rupture and content release above the plane of the membrane. When vesicles rupture above the membrane, the dye contained within diffuses in three dimensions, whereas content release underneath a tethered patch acts as pseudo-2D diffusion (the gap between the solid support and the patch is 8 nm) (11). Previous work from our lab has studied content transfer with calcein-containing vesicles and used mathematical models to describe the kinetics expected for dye diffusion under each of these circumstances (13). Dye diffusion in three dimensions is observed to be much faster than diffusion in two dimensions: upon vesicle rupture, the content dye diffuses away from the site of fusion within 100 ms, whereas pseudo-2D diffusion underneath a tethered patch takes several hundred ms to complete. For the content transfer experiments described here, dye diffusion from the vesicle was complete within ~500–700 ms, consistent with the model for pseudo-2D diffusion (Fig. 6 *C*).

When fusion outcomes were monitored with the content transfer assay, ~1% of events with DNA-lipid on both incoming vesicles and target patch were observed to proceed to full fusion. Similar to lipid mixing experiments, incorporation of a DNA-solanesol anchor into one or both membranes increased the amount of eventual full fusion (Fig. 6 *B*). The asymmetric effect of DNA-solanesol positioning noted in hemi- to full fusion, and thus eventual full fusion, in lipid mixing experiments is less evident here: although 7% full fusion is observed when DNA-solanesol is present in vesicles but not the target patch, this is not a significant increase from the 5% observed with DNA-solanesol present on the target patch but not incoming vesicles. In contrast, when DNA-solanesol is present on both membranes, the amount of eventual full fusion increases to 9%. This increase is consistent with the results obtained from the lipid mixing experiments, wherein the highest amount of eventual full fusion was observed when both vesicles and target patch contained DNA-solanesol. Although higher levels of eventual full fusion were observed in lipid mixing experiments, this may be attributed to the different preparations of vesicles required for the two experiments: SUVs for content transfer are extruded with sulforhodamine dye and

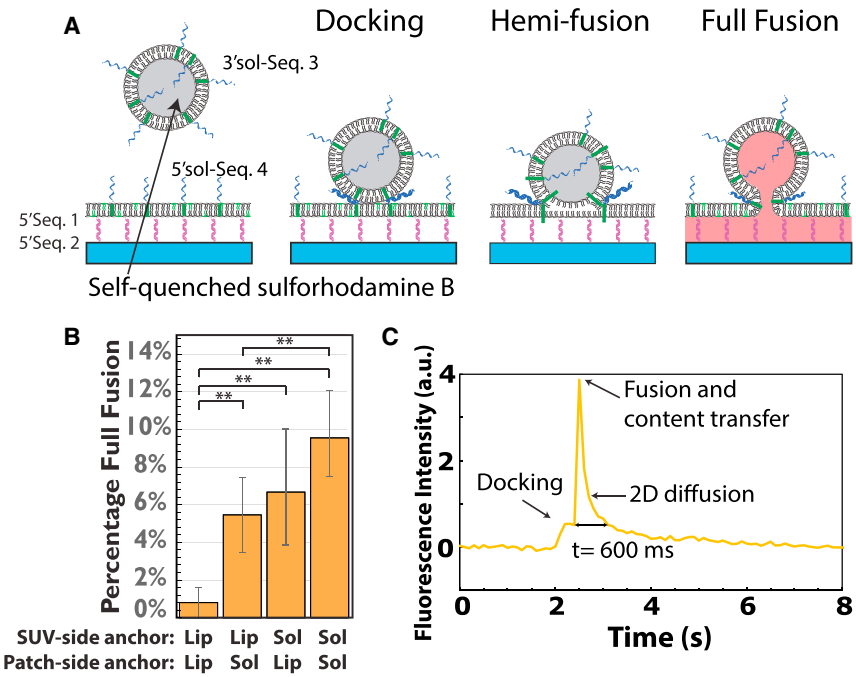

FIGURE 6 DNA-mediated vesicle fusion to tethered patches, monitored by content transfer. (*A*) Given here is a schematic of the content transfer experiment. DNA-sol is anchored in the bilayer at the 3′ end in vesicles and the 5′ end on the target membrane. Vesicles contain SRB at self-quenching concentrations, which allows for visualization of vesicles in the plane of the tethered patch. Full fusion is accompanied by a sharp increase in fluorescence corresponding to SRB dequenching. (*B*) Shown here is the percent of eventual full fusion monitored by content transfer across a tethered membrane mediated by DNA-lipids (*Lip*) and DNA-solanesol (*Sol*). $n > 180$ for all conditions. (*C*) Given here is an example of a fluorescence trace of a full fusion event. There is a small increase in fluorescence as the vesicle docks, followed a sharp increase corresponding to dye dequenching and diffusion over several hundred ms. To see this figure in color, go online.

purified from untrapped dye by size exclusion, whereas SUVs for lipid mixing experiments are used after extrusion with no subsequent purification, as the dye label is incorporated into the lipid mixture. Content transfer showed a lower percentage full fusion than lipid mixing under all conditions investigated.

In conclusion, incorporation of DNA-solanesol into either incoming SUVs or the target tethered patch is sufficient to cause an increase in eventual full fusion. Although incorporation on only one membrane is sufficient to cause an increase in fast full fusion, an asymmetric effect is observed in hemi- to full fusion monitored by lipid mixing, which increases with the presence of DNA-solanesol in incoming vesicles but not in the target patch. This may be indicative that the full fusion and hemi- to full fusion transitions proceed via different pathways. Content transfer experiments also exhibit an increase in full fusion when mediated by DNA-solanesol as compared to the single-leaflet DNA-lipid. Although no drastic increase in full fusion is observed, this is consistent with the low efficiency of spontaneous fusion measured in other model systems with SNARE proteins (8,28–31). Although it is unknown whether solanesol serves as a true transmembrane anchor, it is of sufficient length to interact with both leaflets of the membrane. Our results suggest that the length and hydrophobicity of the anchor contribute to the efficiency of full fusion in our DNA-mediated system, indicating that solanesol plays a role other than that of a passive anchor and may instead provide increased tension on the vesicle and target membrane that leads to fusion.

SUPPORTING MATERIAL

Supporting Materials and Methods, ten figures, and one table are available at http://www.biophysj.org/biophysj/supplemental/S0006-3495(17)30573-8.

AUTHOR CONTRIBUTIONS

K.M.F. and S.G.B. designed the research. K.M.F. performed the research and analyzed the data. K.M.F. and S.G.B. wrote the article. S.G.B. contributed material resources.

ACKNOWLEDGMENTS

We thank Dr. Robert Rawle for his assistance with the single vesicle fusion assay and development of the MATLAB programs used for analysis and quantification. Dr. Bettina van Lengerich developed the syntheses for single-leaflet DNA-lipids and early DNA-transmembrane anchor conjugates. Professor Paul Wender provided advice and suggested the use of the disulfide linkage to conjugate DNA and solanesol.

This work was supported in part by the National Institutes of Health (GM069630 and GM118044) and the National Science Foundation Biophysics Program.

SUPPORTING CITATIONS

Reference (32) appears in the Supporting Material.

REFERENCES

1. Chen, Y. A., and R. H. Scheller. 2001. SNARE-mediated membrane fusion. *Nat. Rev. Mol. Cell Biol.* 2:98–106.
2. Stein, A., G. Weber, …, R. Jahn. 2009. Helical extension of the neuronal SNARE complex into the membrane. *Nature.* 460:525–528.
3. Sutton, R. B., D. Fasshauer, …, A. T. Brunger. 1998. Crystal structure of a SNARE complex involved in synaptic exocytosis at 2.4 Å resolution. *Nature.* 395:347–353.
4. Jahn, R., and D. Fasshauer. 2012. Molecular machines governing exocytosis of synaptic vesicles. *Nature.* 490:201–207.
5. Lai, Y., J. Diao, …, A. T. Brunger. 2014. Complexin inhibits spontaneous release and synchronizes Ca2+-triggered synaptic vesicle fusion by distinct mechanisms. *eLife.* 3:e03756.
6. Chicka, M. C., E. Hui, …, E. R. Chapman. 2008. Synaptotagmin arrests the SNARE complex before triggering fast, efficient membrane fusion in response to Ca^{2+}. *Nat. Struct. Mol. Biol.* 15:827–835.
7. Zhou, P., T. Bacaj, …, T. C. Südhof. 2013. Lipid-anchored SNAREs lacking transmembrane regions fully support membrane fusion during neurotransmitter release. *Neuron.* 80:470–483.
8. Bowen, M. E., K. Weninger, …, S. Chu. 2004. Single molecule observation of liposome-bilayer fusion thermally induced by soluble N-ethyl maleimide sensitive-factor attachment protein receptors (SNAREs). *Biophys. J.* 87:3569–3584.
9. Domanska, M. K., V. Kiessling, and L. K. Tamm. 2010. Docking and fast fusion of synaptobrevin vesicles depends on the lipid compositions of the vesicle and the acceptor SNARE complex-containing target membrane. *Biophys. J.* 99:2936–2946.
10. Karatekin, E., J. Di Giovanni, …, J. E. Rothman. 2010. A fast, single-vesicle fusion assay mimics physiological SNARE requirements. *Proc. Natl. Acad. Sci. USA.* 107:3517–3521.
11. Chung, M., R. D. Lowe, …, S. G. Boxer. 2009. DNA-tethered membranes formed by giant vesicle rupture. *J. Struct. Biol.* 168:190–199.
12. Chan, Y. H., B. van Lengerich, and S. G. Boxer. 2008. Lipid-anchored DNA mediates vesicle fusion as observed by lipid and content mixing. *Biointerphases.* 3:FA17–FA21.
13. Rawle, R. J., B. van Lengerich, …, S. G. Boxer. 2011. Vesicle fusion observed by content transfer across a tethered lipid bilayer. *Biophys. J.* 101:L37–L39.
14. van Lengerich, B., R. J. Rawle, …, S. G. Boxer. 2013. Individual vesicle fusion events mediated by lipid-anchored DNA. *Biophys. J.* 105:409–419.
15. McNew, J. A., T. Weber, …, J. E. Rothman. 2000. Close is not enough: SNARE-dependent membrane fusion requires an active mechanism that transduces force to membrane anchors. *J. Cell Biol.* 150:105–117.
16. Fdez, E., M. Martínez-Salvador, …, S. Hilfiker. 2010. Transmembrane-domain determinants for SNARE-mediated membrane fusion. *J. Cell Sci.* 123:2473–2480.
17. Xu, Y., F. Zhang, …, Y.-K. Shin. 2005. Hemifusion in SNARE-mediated membrane fusion. *Nat. Struct. Mol. Biol.* 12:417–422.
18. Grote, E., M. Baba, …, P. J. Novick. 2000. Geranylgeranylated SNAREs are dominant inhibitors of membrane fusion. *J. Cell Biol.* 151:453–466.
19. Ungermann, C., and D. Langosch. 2005. Functions of SNAREs in intracellular membrane fusion and lipid bilayer mixing. *J. Cell Sci.* 118:3819–3828.
20. Lygina, A. S., K. Meyenberg, …, U. Diederichsen. 2011. Transmembrane domain peptide/peptide nucleic acid hybrid as a model of a SNARE protein in vesicle fusion. *Angew. Chem. Int. Ed. Engl.* 50:8597–8601.
21. Wehland, J.-D., A. S. Lygina, …, U. Diederichsen. 2016. Role of the transmembrane domain in SNARE protein mediated membrane fusion: peptide nucleic acid/peptide model systems. *Mol. Biosyst.* 12:2770–2776.
22. Zhou, Z., and C. J. Fahrni. 2004. A fluorogenic probe for the copper(I)-catalyzed azide-alkyne ligation reaction: modulation of the fluorescence

emission via $3(n,\pi)$-$1(\pi,\pi)$ inversion. *J. Am. Chem. Soc.* 126:8862–8863.

23. Hughes, L. D., and S. G. Boxer. 2013. DNA-based patterning of tethered membrane patches. *Langmuir.* 29:12220–12227.

24. Yoshina-Ishii, C., and S. G. Boxer. 2003. Arrays of mobile tethered vesicles on supported lipid bilayers. *J. Am. Chem. Soc.* 125:3696–3697.

25. Gamblin, D. P., S. van Kasteren, …, B. G. Davis. 2008. Chemical site-selective prenylation of proteins. *Mol. Biosyst.* 4:558–561.

26. Patterson, S. D., and V. Katta. 1994. Prompt fragmentation of disulfide-linked peptides during matrix-assisted laser desorption ionization mass spectrometry. *Anal. Chem.* 66:3727–3732.

27. Chan, Y. H., B. van Lengerich, and S. G. Boxer. 2009. Effects of linker sequences on vesicle fusion mediated by lipid-anchored DNA oligonucleotides. *Proc. Natl. Acad. Sci. USA.* 106:979–984.

28. Diao, J., P. Grob, …, A. T. Brunger. 2012. Synaptic proteins promote calcium-triggered fast transition from point contact to full fusion. *eLife.* 1:e00109.

29. Lai, Y., J. Diao, …, Y.-K. Shin. 2013. Fusion pore formation and expansion induced by Ca^{2+} and synaptotagmin 1. *Proc. Natl. Acad. Sci. USA.* 110:1333–1338.

30. Shi, L., Q.-T. Shen, …, F. Pincet. 2012. SNARE proteins: one to fuse and three to keep the nascent fusion pore open. *Science.* 335:1355–1359.

31. Kiessling, V., S. Ahmed, …, L. K. Tamm. 2013. Rapid fusion of synaptic vesicles with reconstituted target SNARE membranes. *Biophys. J.* 104:1950–1958.

32. Flavier, K. 2016. Vesicle fusion mediated by hybridization of transmembrane-anchored DNA (Doctoral Dissertation). Stanford University, Stanford, CA.

Biophysical Journal, Volume *113*

Supplemental Information

Vesicle Fusion Mediated by Solanesol-Anchored DNA

Kristina M. Flavier and Steven G. Boxer

Supporting Material

Vesicle fusion mediated by solanesol-anchored DNA

Kristina M. Flavier and Steven G. Boxer

Department of Chemistry, Stanford University, Stanford, CA 94305

Contents

1. Single leaflet-spanning DNA-lipids and sequences used

DNA-lipids with the diglycerol ether anchor (Fig. S1) were prepared as previously described (1) via coupling of a diglycerol ether phosphoramidite to the 5' or 3' end of a DNA sequence (Table S1). A 5' or 3' preceding the DNA sequence name demarcates the end of the sequence on which the lipid anchor is present.

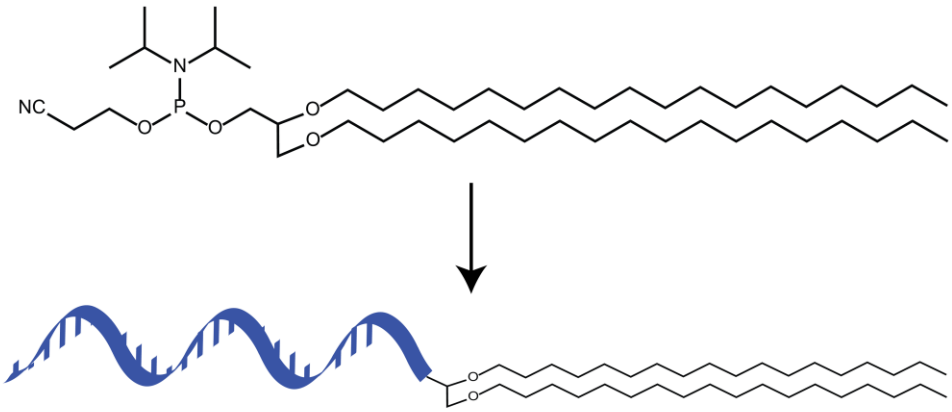

Fig. S1. The diglycerol ether used as the DNA-lipid single leaflet-spanning membrane anchor. The lipid is added to the 5' or 3' terminus of DNA via a phosphoramidite linkage.

Table S1. DNA sequences used on DNA-lipids and DNA-solanesol, listed from 5' to 3'. 5'Sequence 1 was used to tether GUVs to an azide slide displaying 5'alkyne-modified Sequence 2. 3' Sequence 3 and 5'Sequence 4 were used to mediate vesicle fusion.

Name	Sequence
Sequence 1	TGC GGA TAA CAA TTT CAC ACA GGA
Sequence 2	TCC TGT GTG AAA TTG TTA TCC GCA
Sequence 3	TAG TAT TCA ACA TTT CCG TGT CGA
Sequence 4	TCG ACA CGG AAA TGT TGA ATA CTA

2. Synthesis of Alexa 647-Sequence 3 and 5'Sequence 3-Alexa 647 for quantification experiments

DNA sequence 3 containing a terminal amino modifier (20 nmol, 1 equiv.) was dissolved in 50 µL 300 mM sodium bicarbonate (pH 8.2). Alexa 647-NHS ester in 50 µL DMSO (400 nmol, 20 equiv.) was added and the reaction mixture stirred overnight at room temperature. Excess dye was removed by ethanol precipitation of DNA and the product was purified by RP-HPLC and

lyophilized. Alexa 647-Sequence 3 was obtained in 74% yield (15 nmol) as a blue powder and the product identity verified by MALDI-TOF.

5'lipid-Sequence 3 containing a 3' amine modifier was synthesized according to published procedures (1). 5'Sequence 3-amine (9.1 nmol, 1 equiv.) was dissolved in 50 µL 300 mM sodium bicarbonate (pH 8.2). Alexa 647-NHS ester in 23 µL DMSO (180 nmol, 20 equiv.) was added and the reaction mixture stirred overnight at room temperature. DNA-lipid was separated from unconjugated dye by three rounds of purification on a PD-10 column and eluted with pH 7.4 PBS. Fractions containing DNA were combined and dried down to a volume of 400 µL between each round. The final product contained 0.53 nmol of 5' Sequence 3 and 0.26 nmol Alexa 647, as measured by absorbance at 260 and 650 nm respectively, indicating that about 50% of 5' Sequence 3 present in the product was conjugated to Alexa 647 (6% yield). HPLC purification under the conditions previously mentioned for DNA purification further removed free dye, for 74% Alexa 647 labeling in the final product.

3. Quantification of DNA on the exterior of SUVs

To determine the fluorescence intensity of a single dye under the imaging conditions used, a single-molecule photobleaching experiment was conducted. To fuseogenic vesicles containing OG-DHPE and no DNA was added 0.025 mol% 5' Sequence 3-Alexa 647 (corresponding to 3 dyes per 50 nm SUV at a 50% dye conjugation efficiency). Vesicles were incubated with dye-DNA-lipid at 4° C overnight. Single-step photobleaching was used in combination with a custom-written Matlab program to determine the average fluorescence intensity of one Alexa 647 dye (Fig. S2). OG-DHPE was used to select vesicles for quantification. The background of regions containing no vesicles was subtracted from the fluorescence trace of each vesicle, and the total loss of Alexa 647 fluorescence of each SUV was divided by the observed number of photobleaching steps to obtain a distribution of the average fluorescence intensity per dye.

Hybridization of Alexa 647-Sequence 3 with the complementary Sequence 4 displayed on vesicles was used to determine the number of DNA-lipid or DNA-solanesol on the vesicle surface. After extrusion of vesicles containing membrane-anchored Sequence 4, 5 µL of vesicles from the crude product mixture were diluted to 200 µL in PBS. Alexa 647-Sequence 3 (3 equiv) was added and incubated for five hours at room temperature.

Glass coverslips were cleaned in 7X detergent heated to clarity (MP Biomedicals) for 20 min., rinsed with deionized water for two hours, and then baked for four hours at 400° C. Prior to DNA quantification, the cover slips were plasma-cleaned for twenty minutes. A perfusion chamber gasket (Invitrogen) was affixed to the slide. To each chamber was added 100 µL PBS, along with 5 µL of SUVs displaying Alexa 647 diluted to 2 µg/mL. SUVs were incubated on the surface for five minutes and rinsed three times with 100 µL PBS prior to imaging. A custom-written Matlab program was used to measure the fluorescence intensity of Alexa 647 on a selection of vesicles to determine the number of dyes per vesicle. Vesicles were selected based on the presence of OG-DHPE. Background fluorescence intensity of areas not containing vesicles was subtracted from the measured fluorescence intensity of each vesicle, which was then divided by the average fluorescence of one Alexa 647 molecule to obtain an estimate of the number of dyes.

Hybridization of the DNA sequence bearing Alexa 647 to DNA displayed on a membrane was not completely efficient. Upon hybridization to a fully overlapping sequence bearing Alexa 647, the observed number of dyes is approximately 20-30% of the number of DNA expected to be displayed on the surface (Fig. S3). After accounting for this hybridization inefficiency, vesicles

formed with 0.25 mol% 5' lipid Sequence 4 were found to display 14 ± 7 DNA on the surface, equivalent to approximately 43% incorporation. Vesicles formed with 0.25 mol% Sequence 4-solanesol displayed 21 ± 12 DNA on the surface, equivalent to approximately 65% incorporation. For the fusion experiments presented herein, DNA-lipid or DNA-solanesol was incorporated into lipid mixtures prior to rehydration so that they would be present in comparable concentrations in SUVs.

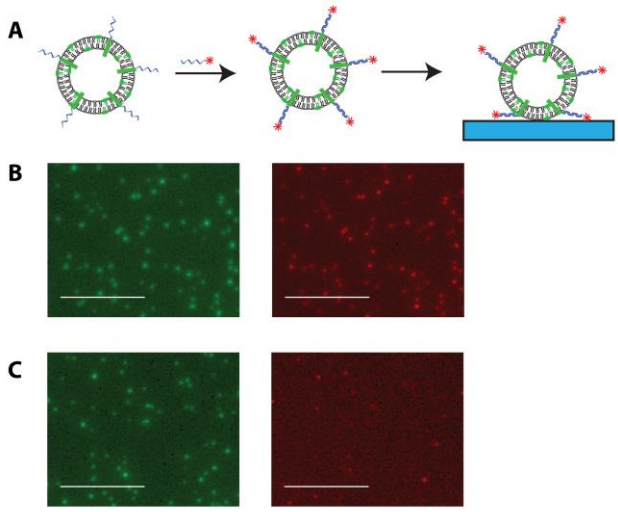

Figure S2. Setup for quantification of the number of DNA on the surface of vesicles. (A) Sequence 4 displayed on the vesicle is hybridized with Alexa 647-Sequence 3. Vesicles are then immobilized on a glass surface and imaged. For calibration experiments with 5' Sequence 3-Alexa 647, dye-DNA-lipid was incorporated into vesicles at the first step and hybridization with a complementary sequence was not performed. (B, C). Example images of Oregon Green (green) and Alexa 647 (red) displayed on vesicles containing 0.25 mol% (B) and 0.02 mol% (C) 5'Sequence 4 per vesicle. Scale bar 10 μm.

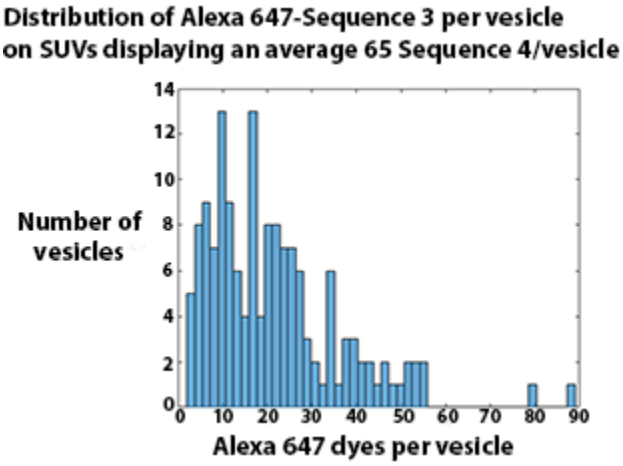

Figure S3. Representative distribution of the number of dyes per SUV observed when 0.25 mol% 5'Sequence 4 was incorporated into the outside of 50 nm SUVs and subsequently hybridized to Alexa 647-Sequence 3. Fluorescence intensity of each dye under the imaging settings used was estimated from single-molecule photobleaching experiments. Mean = 21.5, median = 18.0, n = 150.

4. Quantification of DNA on the surface of GUVs

GUVs were prepared by the gentle hydration method. The lipid mixture used was 2:1:1 DOPC/DOPE/cholesterol, containing 0.5% 5'Sequence 1 to tether, 0.5% Oregon Green-DHPE to aid in locating patches, and 0.5% 5'Sequence 4, 0.1% 5'Sequence 4, 0.5% solanesol-Sequence 4, or no DNA to quantify the number of Sequence 4 displayed on the surface.

The number of solanesol-Sequence 4 displayed on each GUV was estimated via hybridization to the complementary Alexa 647-Sequence 3 sequence, followed by supported lipid bilayer formation and fluorescence quantification (Fig. S4 *A*). After gentle hydration, GUVs were incubated with Alexa 647-Sequence 3 (0.75 mol% relative to lipids) for five hours at room temperature. GUVs were added to glass slides and spontaneously ruptured to form supported lipid bilayers. Images were taken of Oregon Green and Alexa 647 fluorescence for each patch. The average fluorescence intensity of one molecule of Alexa 647 was used to determine the average number of dyes displayed per square micron. Edges of patches and visible defects were avoided for quantification measurements. Efficiency of Alexa 647-Sequence 3 hybridization to membrane-anchored Sequence 4 was estimated assuming that a single leaflet contains approximately one million lipids per square micron, using the typical area for a phospholipid headgroup in a bilayer, roughly 70 $Å^2$. Low hybridization efficiency was observed, with membranes displaying approximately 10% of the expected dye fluorescence, and so a calibration curve was instead used to determine the DNA-sol incorporation efficiency (Fig. S4 *B*).

GUVs with no added Alexa 647-Sequence 3 were ruptured on a glass surface, and the fluorescence per square micron was measured to be about equivalent to 9-10 dyes per μm^2, corresponding to fluorescence in the absence of dye. Alexa 647-Sequence 3 was also added to GUVs that did not display Sequence 4 and the fluorescence intensity per micron upon GUV rupture on glass was measured. This value, approximately 16-18 dyes per μm^2 before subtraction of GUV fluorescence in the absence of dye, was used as the background fluorescence measurement expected for nonspecific interaction of the dye-DNA with the membrane and non-hybridized dye that might remain trapped underneath the SLB upon GUV rupture. The number of dyes/μm^2 due to complementary sequence hybridization was thus obtained by subtracting 17 dyes per μm^2 from the measured fluorescence.

The number of dyes per square micron was plotted against the mole percent DNA-lipid added to vesicles to generate a calibration curve that was used to determine the incorporation efficiency of DNA-solanesol. GUVs containing 0.5 mol% solanesol-Sequence 4 showed less Alexa 647 fluorescence than those containing 0.5 mol% 5'Sequence 4, equivalent to 0.08 mol%, or a 15% incorporation efficiency.

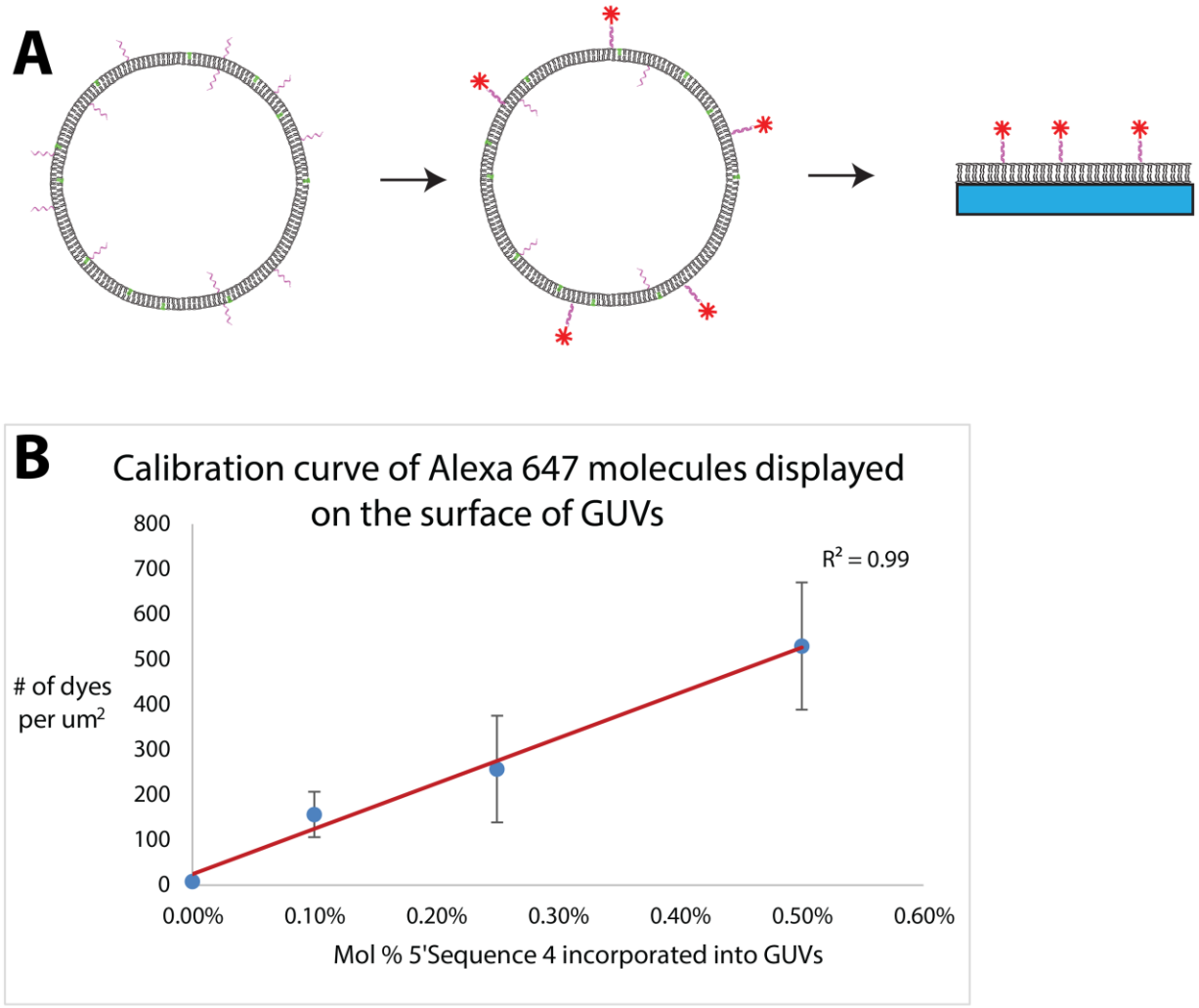

Figure S4. Setup used to determine the incorporation efficiency of solanesol-Sequence 4 into GUVs. (A) GUVs are formed by gentle hydration of lipid mixtures containing 5'lipid-Sequence 4 or solanesol-Sequence 4, then incubated with Alexa 647-Sequence 3 and added to glass to form a supported lipid bilayer. The Alexa 647 fluorescence on the bilayer is then measured. (B) The observed dye fluorescence per square micron fits a linear model. On average, GUVs with 0.5 mol% solanesol-Sequence 4 displayed about 100 dyes/μm^2, or about 0.08 mol% Sequence 4 displayed on the bilayer.

5. Characterization of thiol solanesol

Thiol-solanesol was observed to co-elute with solanesol during column chromatography and a fully pure product was not obtained. As unmodified solanesol itself will not react with activated thiol-DNA, separation of Lawesson's reagent and reaction byproducts was deemed sufficient for use in the subsequent conjugation. When synthesizing primary isoprenoid thiols by this method, tertiary thiol regioisomers may also form as a side product. In prior studies by Gamblin et al., prolonged reaction times increased the proportion of primary thiol obtained: in the case of *trans*-geraniol, a reaction time longer than 20 hours yielded >99% primary thiol, while a reaction time shorter than 6 hours yielded 13% tertiary thiol (2). For this reason, the thionation of

solanesol was conducted over 16-20 hours and NMR used to determine the product composition (Fig. S5). The methine proton of the tertiary thiol product is expected to give rise to a multiplet at 6 ppm, a peak that is not observed in the thiol solanesol product mixture. The thiol solanesol product thus appears to contain less than 1% tertiary thiol.

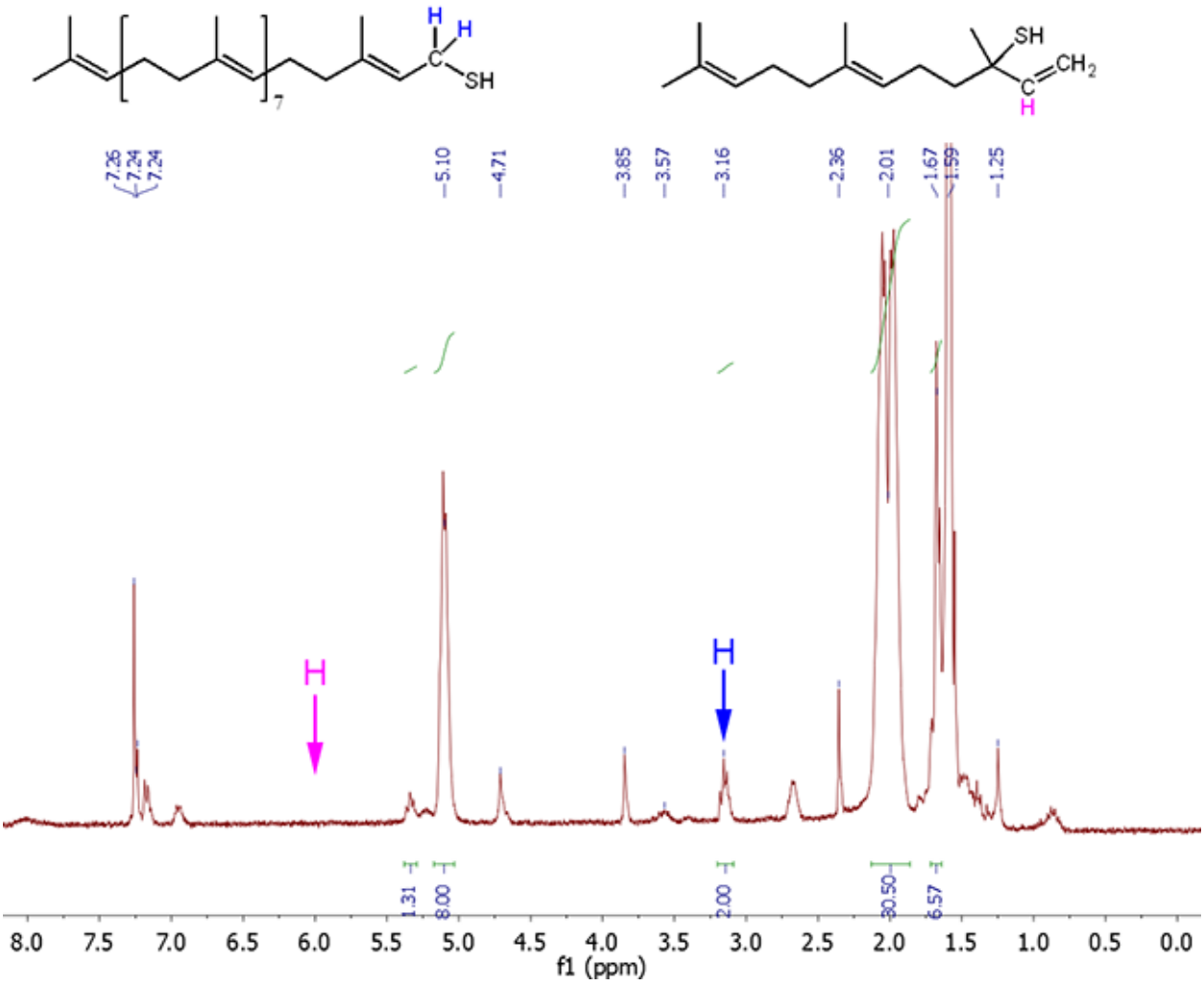

Figure S5. ^{1}H NMR spectrum of thiol-solanesol product in $CDCl_3$. Many of the observed peaks overlap with those expected for solanesol. The apparent triplet at 3.16 ppm (blue) is unique to the desired primary thiol-solanesol product and corresponds to the two protons α to the thiol. No peak is present at approximately 6 ppm (magenta), which would correspond to the methine proton of the tertiary thiol regioisomer.

6. Characterization of DNA-solanesol

RP-HPLC was used to purify the conjugated DNA-solanesol product, which was obtained in 10% yield (Fig. S6).

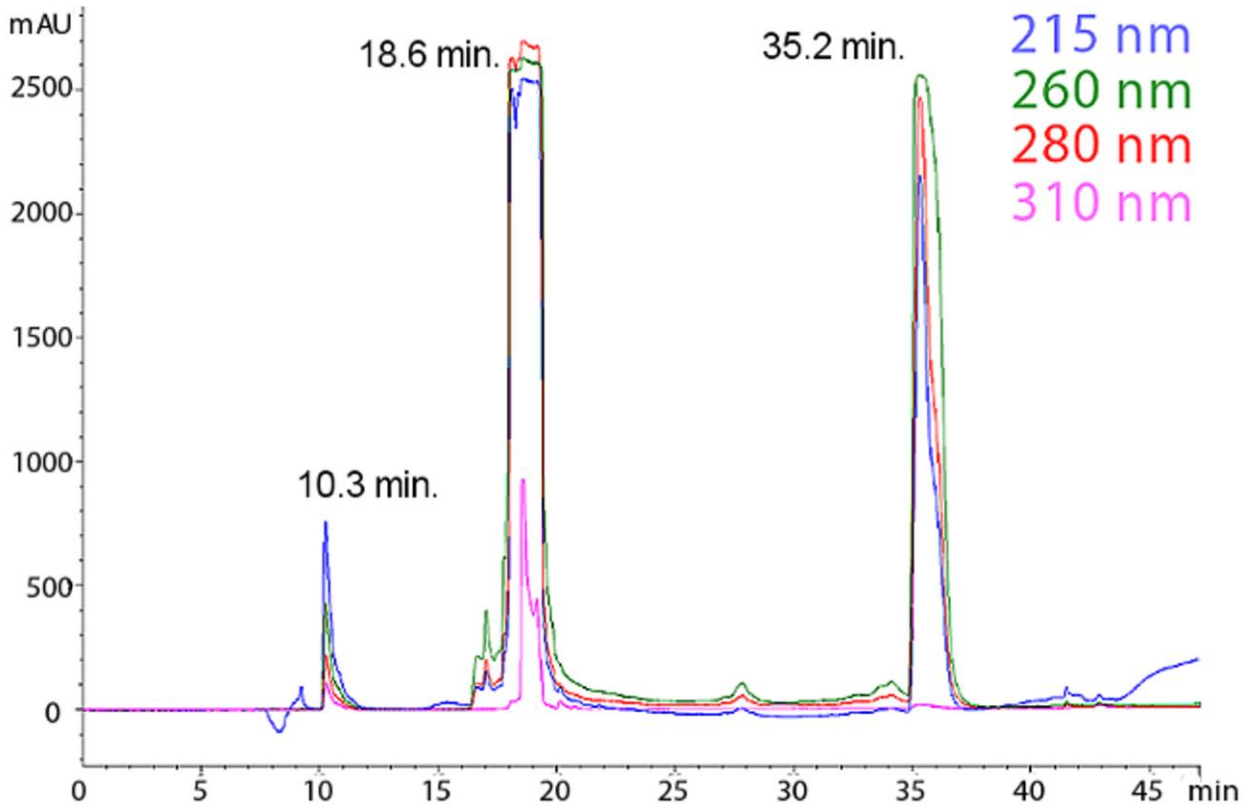

Figure S6. RP-HPLC trace of Sequence 4-solanesol. A clean separation is observed between unreacted activated thiol-Sequence 4 (19 min.) and Sequence 4-solanesol (35 min.). A peak corresponding to free TNB^{2-} (10 min.) is also present.

DNA-solanesol was spotted using 3-HPA as the MALDI matrix and the spectrum showed peaks corresponding to both intact DNA-solanesol and thiol-DNA due to disulfide fragmentation (Fig. S7), which is known to occur in 3-HPA at high laser intensities (3). Fragmentation was not observed in MALDI spectra run in THAP, and the only peak present displays the m/z expected for DNA-solanesol. Taken together, these two spectra confirm that the observed peak is indeed solanesol conjugated to DNA via a disulfide linkage: reduced thiol-DNA is only observed upon disulfide fragmentation of the product.

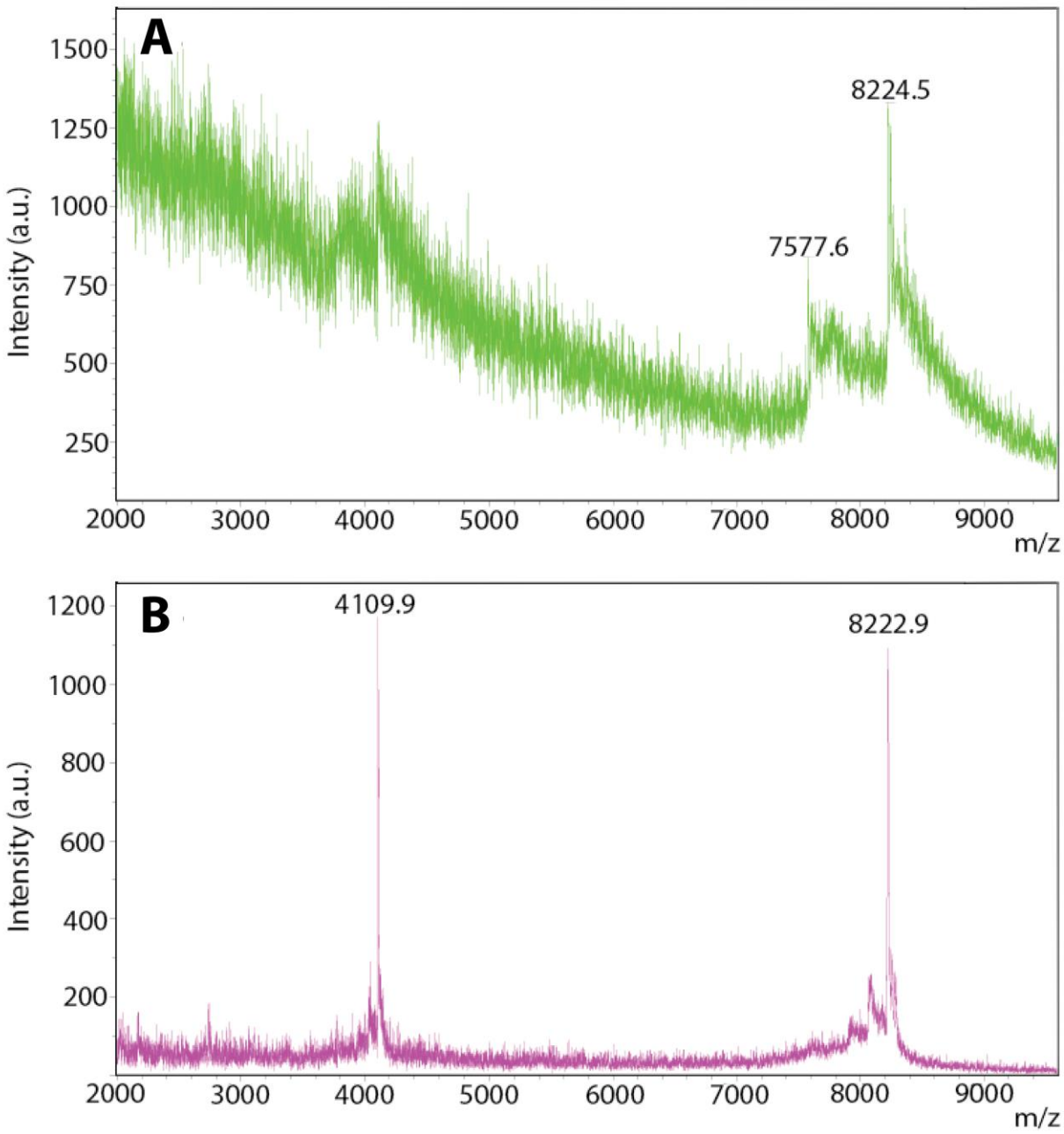

Figure S7. MALDI spectra of Sequence 4-solanesol spotted in (A) 3-HPA and (B) 2,4,6-THAP. Expected MW 8228 Da. Due to disulfide cleavage, the spectrum taken in 3-HPA has lower signal-to-noise ratio and displays a peak corresponding to unconjugated thiol-Sequence 4, expected MW 7581 Da.

7. Alternative DNA-solanesol linkages and transmembrane anchors

In addition to the thiol-solanesol ultimately used as a membrane anchor in these experiments, several other potential anchors were explored. These alternative approaches are discussed in detail in reference 6.

Initial attempts to synthesize a transmembrane-anchored DNA involved conjugation to a peptide derived from the 32 C-terminal amino acids of the synaptobrevin linker and transmembrane domain (Fig. S8 *A*). Two different variants of the peptide were used for these studies: azido-Syb, in which azidolysine (Fig. S8 *B*) was incorporated at the N-terminus for conjugation to DNA via copper-catalyzed and strain promoted click chemistry, and Cys-Syb, in which cysteine was incorporated at the N-terminus for conjugation via disulfide or maleimide chemistries and the interior cysteine was replaced by serine. Conjugation was attempted in solution (carried out in water/methanol or water/acetonitrile mixtures), on solid phase with DNA on resin, or on the surface of SUVs. However, due to the hydrophobicity and low solubility of the transmembrane peptide, the conjugation reactions proceeded in low or no yield. Purification and isolation of the DNA-peptide also proved difficult because of peptide and conjugate aggregation, as well as instability of DNA under the highly acidic conditions optimal for the handling and purification of transmembrane peptides.

Of these approaches, strain-promoted cycloaddition between azido-Syb and dibenzocyclooctyne-DNA (DBCO-DNA) resulted in a conjugate that could be characterized by MALDI and SDS-PAGE. However, the hydrophobic DBCO was found to incorporate into bilayers such that vesicles with DBCO-DNA added into the lipid mixture were observed to tether to membranes displaying the complementary sequence. This necessitated the quantitative removal of DBCO-DNA from the DNA-peptide product prior to its use in fusion experiments, which could not be achieved due to the aforementioned difficulties in conjugate purification.

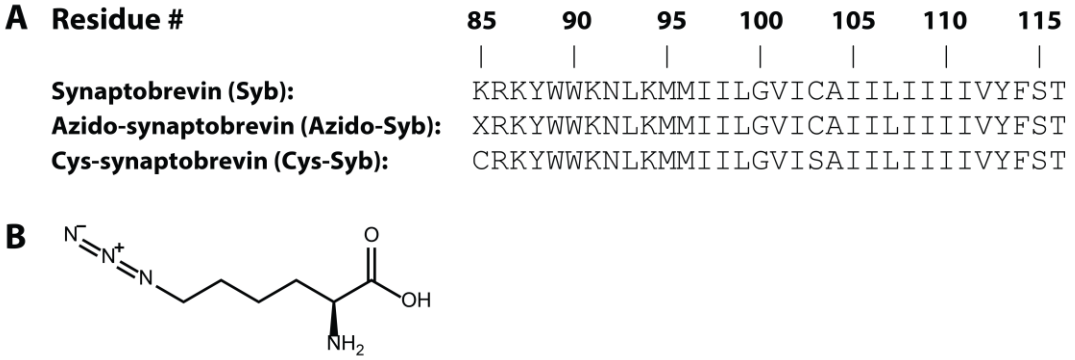

Figure S8. Peptide sequences and reactive functionalities used in DNA-peptide conjugation. (A) Residues 85-116 of synaptobrevin and the transmembrane peptides used for conjugation to DNA, listed from N- to C-terminus. X = azidolysine. (B) Structure of azidolysine, used at the N-terminus of azido-synaptobrevin for conjugation to DNA via click chemistry.

Initially, DNA-solanesol was synthesized via esterification of solanesol with a bifunctional linker that allowed further conjugation to DNA via maleimide or azide-alkyne chemistries (Fig. S9). However, these linkers proved to be unstable under the imaging conditions used for the single-vesicle fusion experiments, possibly due to photocleavage of the allyl ester, which resulted in dissociation of vesicles tethered by hybridized DNA-solanesol away from a membrane displaying the complementary DNA sequence. This dissociation behavior was not observed with DNA-solanesol synthesized via thionation and disulfide linkage described in the main text. The synthesis of DNA-solanesol via esterification to azidoacetic acid, followed by strain-promoted cycloaddition to dibenzocyclooctyne (DBCO)-DNA, is presented here.

To a solution of 9 mg. solanesol (14.3 umol, 1 equiv.) in 4 mL dichloromethane was added 19.2 ug. 4-dimethylaminopyridine (1.6 umol, 0.11 equiv.) and 200 uL azidoacetic acid (2.67 mmol, 190 equiv.). The solution was cooled to 0° C and 3.9 mg. N,N'-dicyclohexylcarbodiimide in 100 uL dichloromethane acetate (18.9 umol, 1.1 equiv.) added dropwise with stirring. The reaction mixture was allowed to warm to room temperature and was stirred at room temperature overnight under positive nitrogen pressure. The product was purified on pipette column in 8:2 hexane/ethyl acetate. While azide-modified solanesyl ester was observed to co-elute with solanesol, separation from unreacted azidoacetic acid was deemed sufficient for subsequent reaction with alkyne-DNA. The product, a mixture of solanesol and azido-solanesol, was obtained as a clear oil.

Azido-solanesol (230.4 nmol, 3 equiv.) was dried down under nitrogen to a thin film and redissolved in 150 uL 1% w/w octylglucoside in water containing DBCO-DNA (76.8 nmol, 1 equiv.). The reaction mixture was incubated at room temperature overnight and the product purified by RP-HPLC. The DNA-solanesol product was obtained as a white powder that was dissolved in water and stored as a stock solution at -20° C (6.8 nmol, 8.9% yield). The product identity was confirmed by MALDI-TOF (Fig. S10).

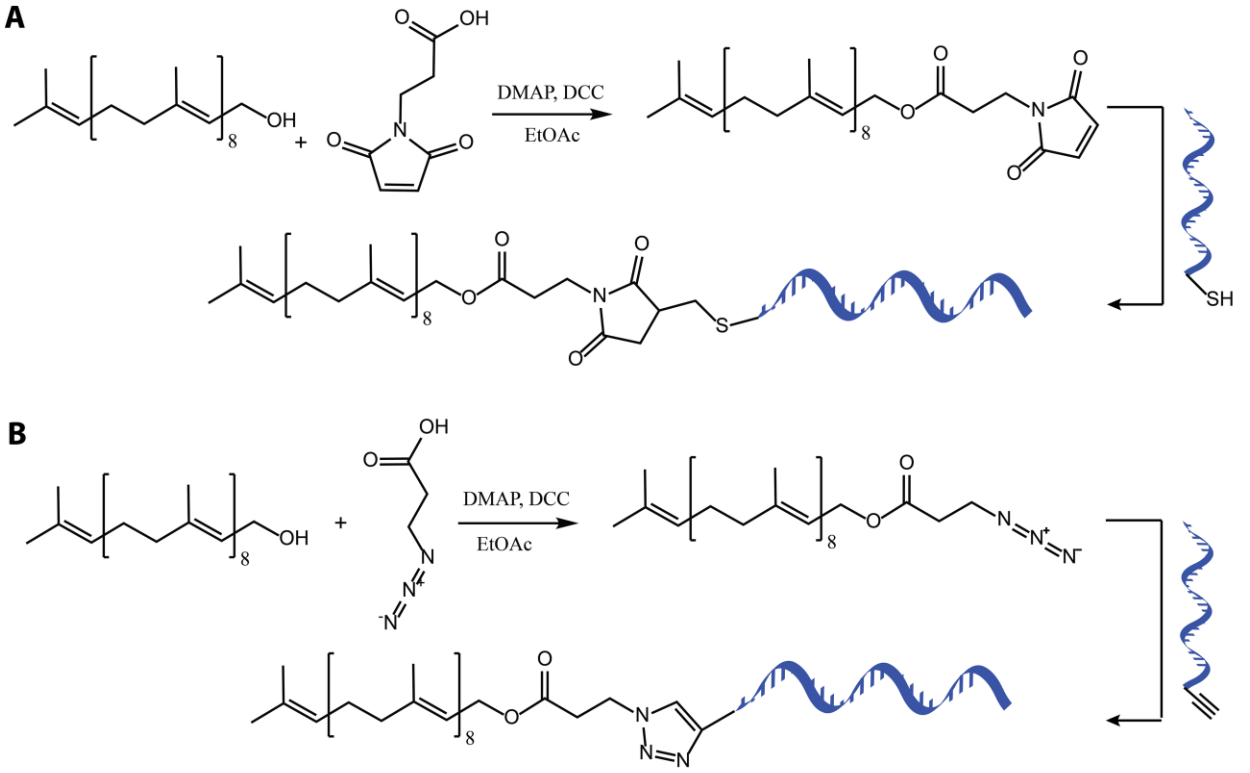

Figure S9. Synthesis of DNA-solanesol via solanesol esterification. (A) Esterification with 3-maleimidopropanoic acid and subsequent reaction with thiol-DNA gives the DNA-maleimide solanesol product. (B) Esterification with azidoacetic acid and subsequent reaction with alkyne-DNA gives the DNA-azide solanesol product.

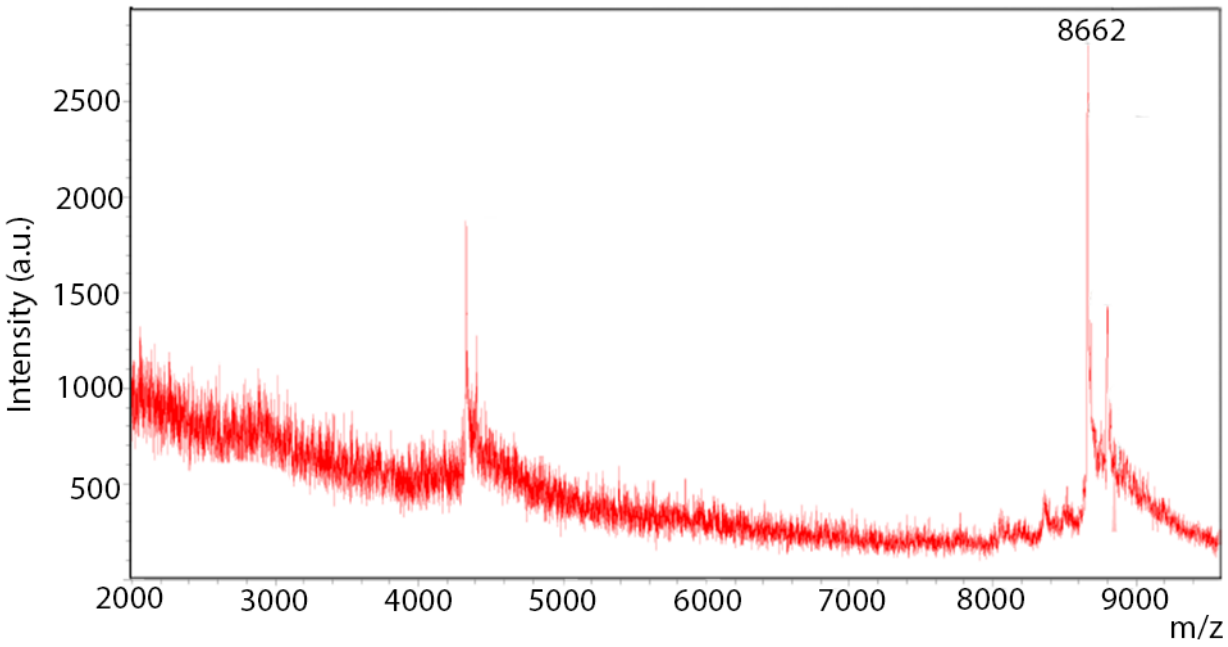

Figure S10. MALDI spectrum of Sequence 4-azido-solanesol. The observed peak has m/z 8662, corresponding to the expected MW of 8669 Da.

8. Control fusion experiments with solanesol-containing membranes mediated by DNA-lipids

To determine whether the presence of the solanesol lipid in the vesicle and target membranes influenced the observed fusion behavior, control experiments were conducted wherein solanesol was incorporated into SUVs and GUVs at the same concentration at which DNA-solanesol was used in each membrane. Fusion experiments mediated by single leaflet-spanning DNA-lipids were then conducted using these solanesol-containing membranes. Solanesol SUVs were added to patches containing no solanesol, while SUVs containing no solanesol were added to patches containing solanesol. In both combinations, the percentages fusion and hemi-to-full fusion observed did not differ significantly from DNA-lipid mediated fusion between membranes not containing solanesol, resulting in approximately 4-5% eventual full fusion.

SUVs for lipid mixing experiments were formed by the extrusion method (4). DNA-lipids to fuse (0.5 mol%) were dried down in a glass vial under stream of nitrogen. The DNA-lipids were then redissolved in chloroform, to which were added 10 µL 2:1:1 DOPC/DOPE/cholesterol at 10 mg/mL in chloroform (0.1 mg), solanesol in chloroform (0.25 mol%, equivalent to the highest concentration of DNA-solanesol used in SUVs), and 4 µL Texas Red-DHPE at 1 mg/mL in chloroform (2 mol%). The mixture was dried down under stream of nitrogen and under vacuum for at least two hours. Lipid films were rehydrated with 250 µL PBS and extruded through a 30 nm polycarbonate filter for an average vesicle diameter of approximately 50 nm (5).

GUVs for tethered patches were formed via the gentle hydration method. The appropriate amounts of DNA-lipids for patch formation and fusion desired in the final GUVs were dried down in a glass vial under stream of nitrogen, equivalent to 0.5 mol% of the sequence to tether the patch and 0.5 mol% of the sequence to fuse. The DNA-lipids were redissolved in chloroform, to which were added 10 µL 2:1:1 DOPC/DOPE/cholesterol at 10 mg/mL in chloroform (0.1 mg), solanesol

in chloroform (0.5 mol%, equivalent to the highest concentration of DNA-solanesol used in patches), and 80 µL Oregon Green-DHPE at 0.01 mg/mL in chloroform (0.5 mol%). The lipid mixture was then dried under stream of nitrogen and under vacuum for at least three hours. To the lipid film was added 200 µL of 500 mM sucrose and the lipids incubated at 37° C for one hour. After pre-incubation, a further 2 mL 500 mM sucrose was added and the GUVs formed by five-hour incubation at 37° C on a platform shaker.

9. Supporting References

1. Chan, Y. H., van Lengerich, B., and Boxer, S. G. 2008. Lipid-anchored DNA mediates vesicle fusion as observed by lipid and content mixing. Biointerphases 3:FA17-FA12.
2. Gamblin, D. P., van Kasteren, S., Bernardes, G. J. L., Chalker, J. M., Oldham, N. J., Fairbanks, A. J., and Davis, B. G. 2008. Chemical site-selective prenylation of proteins. Mol. Biosyst. 4:558-561.
3. Patterson, S. D., and Katta, V. 1994. Prompt fragmentation of disulfide-linked peptides during matrix-assisted laser desorption ionization mass spectrometry. Anal. Chem. 66:3727-3732.
4. Yoshina-Ishii, C., and Boxer, S. G. 2003. Arrays of Mobile Tethered Vesicles on Supported Lipid Bilayers. J. Am. Chem. Soc. 125:3696-3697.
5. van Lengerich, B., Rawle, R. J., Bendix, P. M., and Boxer, S. G. 2013. Individual vesicle fusion events mediated by lipid-anchored DNA. Biophys J. 105:409-419.
6. Flavier, K. 2016. Vesicle fusion mediated by hybridization of transmembrane-anchored DNA (Doctoral dissertation). Stanford University, Stanford.